A Generalized Phase Correction Technique for EPI-PROPELLER

N. Rangwala[1,2], and X. J. Zhou[2,3]

[1]Department of Bioengineering, University of Illinois at Chicago, Chicago, Illinois, United States, [2]Center for Magnetic Resonance Research, University of Illinois Medical Center, Chicago, Illinois, United States, [3]Departments of Radiology, Neurosurgery and Bioengineering, University of Illinois Medical Center, Chicago, Illinois, United States

INTRODUCTION: PROPELLER (Periodically rotated overlapping parallel lines with enhanced reconstruction [1]) based on echo planar imaging (EPI) [2,3] can acquire wider blades with increased time efficiency compared to fast-spin echo (FSE)-based PROPELLER [4]. However, EPI-based sequences suffer from Nyquist ghosts arising primarily from eddy currents and gradient anisotropy [5], thus requiring phase corrections. Although phase errors can be corrected using a reference scan for each blade, this approach can greatly compromise the data acquisition efficiency. A time-efficient phase correction technique based on only two reference scans was recently reported [6]. It has been shown that the technique can reduce the Nyquist ghosts as effectively as the method employing blade-specific reference scans. Additionally, the technique is also capable of reducing oblique Nyquist ghosts (ONG) [7,8] originating from gradient anisotropy. (We call the phase error arising from gradient anisotropy "oblique" phase error).

While the concept of the phase correction technique has been illustrated in the specific case of axial scans, there is a need to generalize the technique for arbitrary imaging planes, including oblique planes. For oblique planes, the ONG can be accentuated, which imposes greater challenges on the phase correction technique. The goal of this study was to develop and demonstrate a generalized phase correction method addressing constant, linear and "oblique" phase errors all together, for any arbitrary imaging plane in EPI-PROPELLER.

List of Equations

$$\begin{bmatrix} G_{ro_x} & G_{pe_x} & G_{sl_x} \\ G_{ro_y} & G_{pe_y} & G_{sl_y} \\ G_{ro_z} & G_{pe_z} & G_{sl_z} \end{bmatrix} = \begin{bmatrix} a_0 & a_1 & a_2 \\ a_3 & a_4 & a_5 \\ a_6 & a_7 & a_8 \end{bmatrix} \begin{bmatrix} \cos\theta & -\sin\theta & 0 \\ \sin\theta & \cos\theta & 0 \\ 0 & 0 & 1 \end{bmatrix} \begin{bmatrix} G_{ro} \\ G_{pe} \\ G_{sl} \end{bmatrix} \quad (1)$$

$$c_\theta \propto (a_0\cos\theta + a_1\sin\theta)c_\parallel + (a_3\cos\theta + a_4\sin\theta)c_\perp + (a_6\cos\theta + a_7\sin\theta)c_\odot \quad (2)$$

$$l_\theta \propto (a_0\cos\theta + a_1\sin\theta)^2 l_\parallel + (a_3\cos\theta + a_4\sin\theta)^2 l_\perp + (a_6\cos\theta + a_7\sin\theta)^2 l_\odot \quad (3)$$

$$o_\theta \propto \frac{\sin 2\theta}{2}\{(a_1^2 - a_0^2)l_\parallel + (a_4^2 - a_3^2)l_\perp + (a_7^2 - a_6^2)l_\odot\} - \cos 2\theta\{a_0 a_1 l_\parallel + a_3 a_4 l_\perp + a_6 a_7 l_\odot\} \quad (4)$$

METHODS: Our correction method relies on three reference scans, each along one of the three orthogonal physical axes: X, Y, and Z. From each reference scan, a constant (c) and a linear (l) phase error are obtained and denoted by ($c_\parallel$, $l_\parallel$), ($c_\perp$, $l_\perp$), and ($c_\odot$, $l_\odot$) for the X-, Y-, and Z-axis, respectively. For an EPI-PROPELLER blade (blade angle = θ) acquired in an arbitrary imaging plane defined by the rotation matrix a, the components of the readout (G_{ro}), phase encoding (G_{pe}) and slice selection (G_{sl}) gradients along the physical X, Y and Z gradient axes are given by Eq. (1). For this blade, the constant (c_θ) and linear (l_θ) phase errors in the readout direction can be derived using Eqs. (2) and (3), respectively, and the "oblique" phase error (o_θ) in the phase-encoding direction [8] can be calculated from Eq. (4).

The generalized phase correction technique was implemented in both long- and short-axis PROPELLER sequences (LAP-EPI [2] and SAP-EPI [3], respectively) on a 3.0 T GE Signa HDx scanner (GE Healthcare, Waukesha, WI). Phase corrections were first evaluated on a square phantom (with 6 cm sides) filled with 100% acetone to reduce the dielectric resonance effect. Three orthogonal reference scans were acquired along the X-, Y- and Z-axis, respectively, followed by the acquisition of a LAP and a SAP dataset in a plane 45° from the axial plane, which formed a rectangle with one side larger than the other by a factor of √2. The following imaging parameters were used: TR = 4000 ms, TE = 65 ms, bandwidth = ±62.5 kHz, acquisition matrix of 128 readout points × 32 phase-encoding steps for LAP and 32 readout points × 128 phase-encoding steps for SAP, number of blades = 6, NEX = 4, FOV = 22 cm, and slice thickness = 5 mm. The raw data were phase-corrected using the technique described above, prior to PROPELLER image reconstruction [1]. The phase correction technique was further evaluated on three healthy male volunteers on a section ~40° from the axial plane, along the preoccipital notch, using both SAP and LAP with similar scan parameters (matrix size = 256, SAP: readout points = 24 and blades = 16, LAP: phase-encoding steps = 16 and blades = 24, FOV = 30 cm). Image acquisition was also performed in other arbitrary planes. The intensity of the Nyquist ghost (g) before and after phase correction was evaluated as a ratio of the mean ghost intensity in a region of interest (ROI; ~100 pixels for the phantom, ~250 pixels for the volunteers) over the signal intensity of a uniform ROI selected within the object.

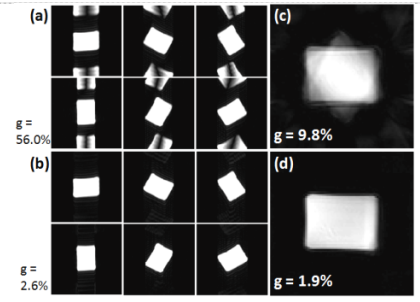

Fig. 1. Individual blades (a,b) and reconstructed LAP-EPI images (c,d) before (a,c) and after (b,d) applying the phase correction technique.

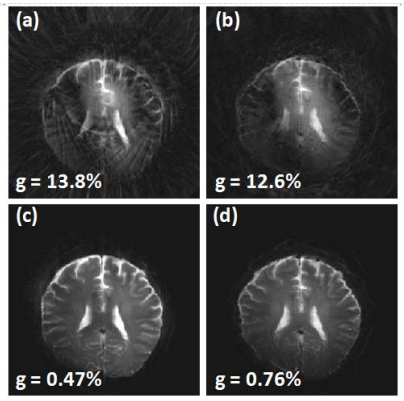

Fig. 2. LAP-EPI (a,c) and SAP-EPI (b,d) in an oblique plane before (a,b) and after (c,d) phase correction on volunteer data. The residual non-uniformity in (c,d) is most likely due to off-resonance caused by sub-optimal shimming.

RESULTS: Figure 1 illustrates the performance of the phase correction technique on the phantom. The left two sub-figures show individual blades of a LAP-EPI dataset before (Fig. 1a) and after (Fig. 1b) applying the phase correction technique. On average, the Nyquist ghosts decreased from 56.0% to 2.6%. In the SAP-EPI dataset (image not shown), the average ghost reduction was from 31.0% to 1.7%. Figures 1c and d show the images reconstructed from Figs. 1a and b, respectively, with the ghost reduced from 9.8% (14.3% for SAP) to 1.9% (1.4% for SAP) after applying the phase correction technique. Figure 2 shows the phase correction applied to data obtained from a human volunteer for both LAP (left column) and SAP (right column). The ghost decreased from 13.8% to 0.47% (Figs. 2a,c) for LAP, and from 12.6% to 0.76% for SAP (Figs. 2b,d). In addition, the phase-related image non-uniformity was also greatly reduced. Other volunteer studies showed similar results (images not shown).

DISCUSSION AND CONCLUSION: The generalized phase correction technique works well for both SAP- and LAP-EPI images in arbitrary planes. The technique has reduced ghosts arising from constant, linear and "oblique" phase errors by at least 80%, obviating the need to acquire a reference scan for each blade. The oblique ghost, which was stronger in an oblique plane (*see* Fig. 1a) compared to that in an "orthogonal" plane, was effectively reduced after applying the ONG correction (Eq. (4)). This technique worked uniformly well under several sub-optimal imaging conditions, such as B_0 and B_1 field non-uniformity. It is also compatible with multi-slice acquisitions with no further increase in the acquisition time of reference scans. Future work involves the application of this technique to anatomically challenging regions such as the heart and the spine.

REFERENCES: [1] Pipe, MRM 1999, 42:963. [2] Wang, *et al.*, MRM 2005, 54:1232. [3] Skare, *et al.*, MRM 2006, 55:1298. [4] Pipe, *et al.*, MRM 2002, 47:42. [5] Aldefeld, *et al.*, MRM 1998, 39:606. [6] Rangwala, *et al.*, ISMRM 2009, p.3100. [7] Reeder, *et al.*, MRM 1999, 41:87. [8] Zhou, *et al.*, ISMRM 1996, p.1477.